Journal of New Materials for Electrochemical Systems 17, 113-122 (2014)

A Kinetic Study of The Hydrogen Evolution Reaction in Phosphoric Acid Solutions with Iron and Manganese Phosphatized Steel Cathodes

G. Alvarado-Macías, J.C. Fuentes-Aceituno* and A. Salinas-Rodríguez

Centro de Investigación y de Estudios Avanzados del IPN, Unidad Saltillo,
Av. Industria Metalúrgica # 1062, Parque Industrial Ramos Arizpe, Ramos Arizpe, Coahuila, 25900, México.

Received: October 31, 2013, Accepted: February 12, 2014, Available online: April 15, 2014

Abstract: *In this investigation a kinetic study of the HER was carried out employing a steel rotating disk with different aqueous solutions containing Phosphoric Acid (H_3PO_4) with or without metallic manganese (Mn) and Nitric Acid (HNO_3). Furthermore, the HER was evaluated on iron and manganese phosphate coatings. Analyses of Tafel plots and the charge transfer coefficients, revealed one electrical potential zone where the monoatomic hydrogen can be recombined electrochemically to H_2 as the rate determining step, with charge transfer coefficients similar to an activationless process ($\alpha \rightarrow 0$). On the other hand, an increase in the concentration of H_3PO_4 promotes a higher exchange current for the HER. The Mn in the aqueous solutions has a catalytic effect on the hydrogen generation rate at room temperature. However, the precipitation of $Mn_3(PO_4)_2$ on steel decreases the HER kinetics at high temperatures. These observations are also supported with SEM (Scanning Electron Microscopy) characterizations.*

Keywords: Polarization, Tafel, monoatomic hydrogen, HER.

1. INTRODUCTION

Hydrogen, as a high-quality clean and renewable energy resource, is increasingly considered as one of the most promising candidates for the fuel of the future [1,2].

Hydrogen evolution reaction (HER) in aqueous solution is one of the most often studied electrode reactions [3,4].

During the last decades, it has been well established that (HER) occurs via two successive elementary events. The initial discharge of hydrogen ions to adsorbed monoatomic hydrogen (equation 1) [5].

$$H^+ + e^- \leftrightarrow H\bullet \quad (1)$$

Followed by the chemical (equation 2) or electrochemical (equation 3) recombination of monoatomic hydrogen to molecular hydrogen.

$$2H \rightarrow H_2 \quad (2)$$

$$H^+ + H\bullet + e^- \rightarrow H_2 \quad (3)$$

*To whom correspondence should be addressed:
Email: juan.fuentes@cinvestav.edu.mx
Phone: 8444389600, Ext 8512

It is well known that water electrolysis is an important technique for hydrogen generation [6]. Although, water electrolysis is not the cheapest method of hydrogen production, it supplies hydrogen of a very high purity in large quantity. Unfortunately, the high energy consumption mainly caused by HER overpotential restrains its application at the present days [7]. One proposed alternative to solve this problem is to use noble metals (such as Pt, Au) as cathode materials for the HER [8]. However, these metals are not only expensive, actually the platinum and gold worldwide reserves are limited [9].

On the other hand, other metallic electrodes such as steels are commonly employed for water electrolysis but these are very susceptible to corrosion effects and consequently their life time is decreased [1]. In this sense, other authors have proposed the use of new and cheap cathode materials resistant to corrosion, for example: the aluminum, Inconel alloys and glassy carbon, however the latter has a very low electrical conductivity, therefore the energy consumption is high [5]. Furthermore, the temperature is one of the variables that strongly affects the corrosion behavior of metallic materials and is widely studied in corrosion investigations and for that reason this variable is also studied in this research [10-15].

Another alternative to reduce the corrosion effects relies on the protection of steel cathodes against corrosion employing the iron

and zinc phosphatizing process [16]. Therefore, this research studied the effect of iron and manganese phosphate coatings on steel on the HER mechanism and kinetics. It was also evaluated the effect of the manganese ion on the HER.

For that reason, the main objective of this research was to understand the nature of HER on different phosphatizing solutions, to determine the different potential regions and solution conditions for carrying out the HER with different phosphatized cathodes.

2. EXPERIMENTAL

2.1. Pre-treatment of the substrate surface

Steel disk electrodes of 10 mm diameter and 0.8 mm thick were prepared with the chemical composition given in Table 1. The sample was mounted in a Teflon support using silver paint connected to a copper wire as an electrical conductor.

The steel samples were conditioned in different ways to be used later in the electrochemical tests: linear polarization (Tafel curves) using the following procedures:

Samples tested were polished to a mirror like finish. Initially, samples were ground on SiC paper of various grain sizes followed by a polishing with Al_2O_3 powder of 0.1 microns and then washed with alcohol. Finally, the samples were glued to a Teflon support using silver paint.

All samples after pre-treatment were immediately phosphatized by immersion in different phosphatizing solutions.

2.2. Phosphatizing process and hydrogen generation tests

Different phosphatizing solutions were tested, which were prepared with phosphoric Acid (85.8 %, J. T. Baker) metallic manganese (99.99 %, Aldrich), Nitric Acid (65.7 %, J. T. Baker), Sodium Hydroxide (97%, J.T. Baker) and distilled water (Jalmek). These solutions were prepared varying the concentrations of H_3PO_4 and Mn with and without the presence of catalyst (HNO_3) at 25, 50, 80 and 90 °C. Table 2 shows in detail the conditions of the various solutions studied:

It is worth to mention that the phosphatizing solutions A and B were used in order to produce the iron phosphate coating on the steel disk electrode. On the other hand, Solution C was employed to generate an iron phosphate coating on the steel with the presence of Mn ion in solution. Finally Solution D was used to form the manganese phosphate coating on the steel disk electrode. These solutions were employed in order to study the effect of the phosphatizing solution (varying acidity with and without the presence of Mn ions or HNO_3 as catalyst), temperature and type of coating (iron or manganese phosphate) on the hydrogen evolution reaction kinetics.

Table 1. Chemical composition of the steel disk.

Si 0.247 %	Mn 0.452 %	Cr 1.02 %
Ni 0.075 %	Mo 0.885%	V <0.0004 %
Cu 0.101 %	Al 0.014 %	Ti 0.004 %
Nb 0.035 %	C 0.280 %	S 0.061 %

Table 2. Phosphatizing solutions.

Solution	H_3PO_4 ($mol \cdot L^{-1}$)	Mn ($mol \cdot L^{-1}$)	HNO_3 ($mol \cdot L^{-1}$)	Temperature (ºC)	pH
A	0.47	-	-	25, 50, 80, 90	-
B	0.94	-	-	25, 50, 80, 90	-
C	0.94	0.6	-	25, 90	1
D	0.94	0.6	0.2	90	2.57

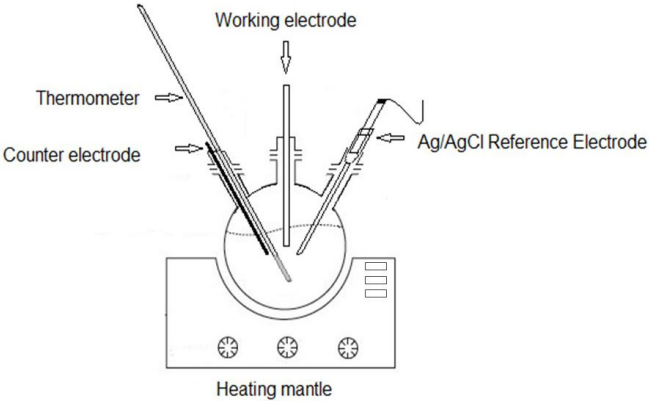

Figure 1. Single-Chamber, three-electrodes electrochemical cell for the phosphatizing experiments.

The phosphatizing and the HER tests were carried out in a conventional three electrodes electrochemical cell (see Figure 1). The cell consisted of a 250 mL round-bottomed flask, instrumented with a thermometer, a Ag/AgCl reference electrode (Thermo Scientific Orion) in contact with the solution through a Luggin capillary, a high purity graphite rod (Alfa Aesar) as a counter electrode and a port to place the working electrode (steel sample). The electrochemical cell was placed in a heating mantle.

The procedure used to study the phosphatizing process along with the HER was as follows: the prepared phosphatizing solution was placed (200 mL) in the electrochemical cell (Figure 1), then the solution was heated to the desired temperature (from 25 to 90 °C), once the thermal equilibrium was reached, the working electrode was immersed (steel sample) and connected to the potentiostat PGZ301 (VoltaLab). Polarization curves were recorded in the cathodic direction every four minutes during 24 min of the immersion process. The linear polarization curves were performed, sweeping the potential at $10mV \cdot s^{-1}$ from - 700 mV to 50 mV vs Ag/AgCl at different temperatures. In order to study the HER kinetics, data obtained from E vs. i (current vs. potential) curves in the cathodic direction were converted to E vs log i, better known as Tafel curves. The corrosion potential (E_{corr}) was also calculated in the different acid solutions H_3PO_4 using the VoltaMaster software.

At the end, the phosphatized steel sample was withdrawn (working electrode), rinsed with distilled water and then it was morphologically and chemically characterized by the Scanning Electron Microscopy (SEM) technique (Phillips, Model: XL30ESEM) taking secondary electron images and X-ray energy dispersion spectroscopy (EDXS) respectively.

3. RESULTS AND DISCUSSION

As was mentioned before, the polarization behavior of hydrogen

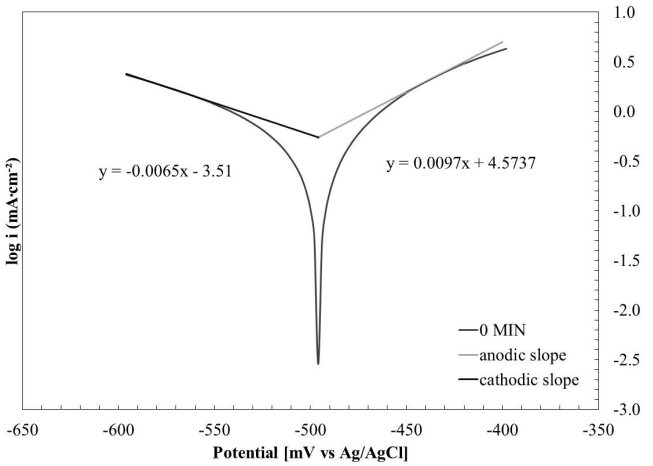

Figure 2. Typical polarization curve or Tafel plot, representing the Tafel lines for an anodic and a cathodic process.

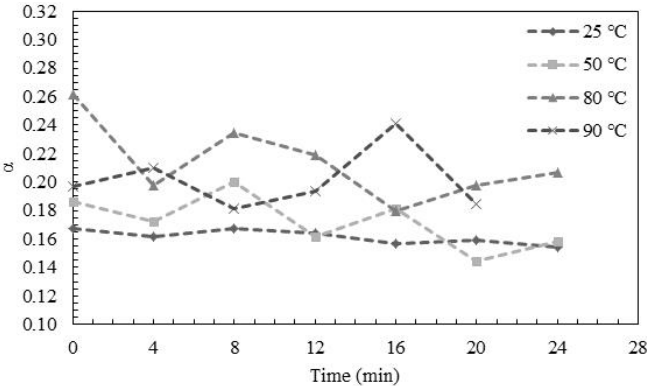

Figure 3. Comparison of charge transfer coefficient (α) at different temperatures and processing times in an aqueous 0.47 M H_3PO_4 solution.

evolution reaction was studied on all cathodes (steel coated with iron or manganese phosphate) employing a three electrodes electrochemical cell; varying acidity, temperature and composition in the phosphatizing solution. It is also shown the polarization behavior on the steel cathodes in the presence of manganese ions.

Before presenting the results it is important to show the shape of the expected polarization curves. Figure 2 shows a typical polarization curve, or complete Tafel plot with the anodic and cathodic Tafel slopes.

The Tafel slope (b') obtained in a polarization curve corresponds basically to three types of processes, which represent a controlling discharge reaction: barrierless with (α=1), ordinary discharge with (α=0.5) and activationless discharge with (α=0) [5,9].

The physical meaning of these types of processes relies on the magnitude of the activation energy in the discharge reaction, in other words when the activationless process occurs (α=0), it indicates that the activation energy for the electrochemical reaction is the smallest possible, which means in kinetic terms that the reaction occurs at the fastest rate [5, 17].

3.1. Effect of the acidity at different temperatures without Mn in solution

Figure 3 presents the charge transfer coefficients for a 0.47 M H_3PO_4 solution at different temperatures (25, 50, 80, 90°C); these charge transfer coefficients (α) were obtained from a Tafel analysis of Figure 4, employing the next equation (equation 4), where (b') represents the slope term in the Tafel equation, R = the universal gas constant, T= the temperature, n= the number of electrons transferred in an electrochemical reaction and F= the Faraday constant:

$$b' = \frac{RT}{\alpha nF} \tag{4}$$

It is interesting to note, that the charge transfer coefficients remain almost constant during the 24 min of the phosphatizing process in a range from 0.16 to 0.26. These charge transfer coefficients are representative of an activationless process (α→0), suggesting a low activation energy for the HER.

Experimental polarization curves for the hydrogen evolution reaction at different acidity (0.47 and 0.94 M H_3PO_4) and temperature are shown in Figure 4 and 6 respectively.

Figure 4 shows the cathodic polarization curves for a 0.47 M H_3PO_4 solution at 25°C, 50°C, 80°C, 90°C (Figures 4A, 4B, 4C, and 4D, respectively) this polarization curves were registered every 4 min during 24 min of immersion.

Figure 4A shows that the HER kinetics was slow at time 0 due to the steel surface was clean (without any layer on it) and when the immersion time passed the hydrogen production rate raised due to the formation of an iron phosphate coating on the steel and this type of coating favors the HER kinetics. For example this behavior can be observed in Figure 4A at a potential of -560mV vs Ag/AgCl where the current density is increased at higher processing times than 0 min. Furthermore the exchange current density (i_0) is increased while the phosphatizing process proceeds (see Table 3). On the other hand, it is worth to mention that the exchange current density can be also related to the steel corrosion rate; however, this is only possible to occur at the beginning of the phosphatizing process i.e. (at 0 min), where the steel corrosion takes place at the highest rate. The corrosion mechanism is shown in the next equations (see equation 5 and 6):

Oxidation of the iron contained in the steel (equation 5)

$$Fe^0 \rightarrow Fe^{+2} + 2e^- \tag{5}$$

Protons reduction to molecular hydrogen (equation 6)

$$2H^+ + 2e^- \rightarrow H_2 \tag{6}$$

However the phosphatizing process begins almost immediately after the steel is corroded, according to Alvarado-Macías et al (2013) [16]. Therefore the increase found in the exchange current density at processing times bigger than 0 is related to the hydrogen production. (Table 3).

Furthermore, Tafel slopes (b') in all cases are very similar (see Table 3A), according to Fuentes-Aceituno and Lapidus (2012) [5], this behavior suggests that the same type of HER mechanism is taking place, the most probable mechanism that is occurring in these type of systems can be a slow electrochemical recombination

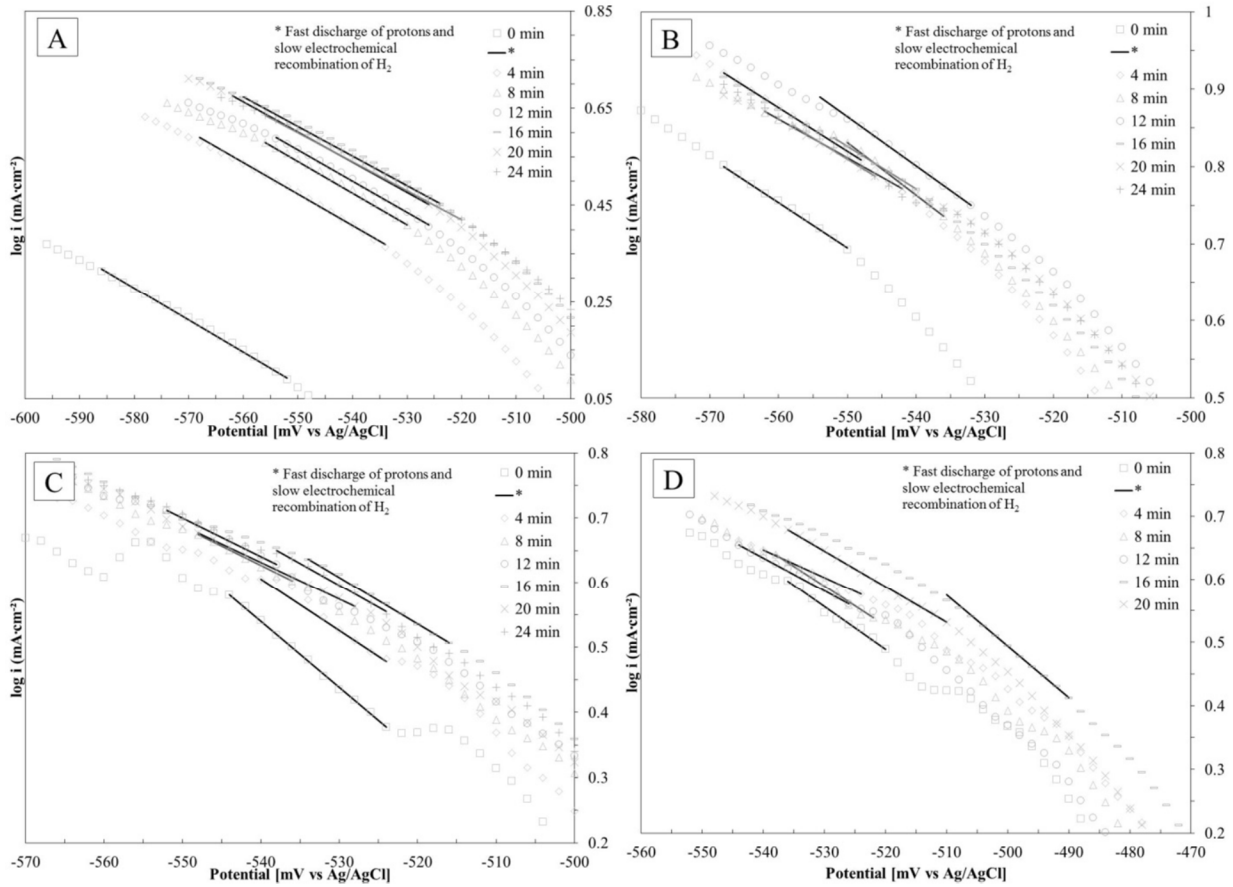

Figure 4. Comparison of the cathodic polarization curves for immersion of steel in an aqueous H_3PO_4 solution at A)25°C, B)50°C, C)80°C, D)90°C. All experiments employed 0.47 M H_3PO_4. The polarization curves were recorded every 4 minutes during the immersion process.

Table 3. Kinetic parameters for the electrochemical recombination rate-controlling step, employing an aqueous 0.47M H_3PO_4 solution. A) 25°C, B) 50°C, C) 80°C, D) 90°C.

A)

Time (min)	b' (V/decade)	i_0 (mA·cm^{-2})	A
0	-0.116	0.882	-4.092
4	-0.154	1.133	-2.936
8	-0.130	1.133	-3.512
12	-0.139	1.139	-3.249
16	-0.169	1.221	-2.532
20	-0.154	1.221	-2.894
24	-0.147	1.133	-3.025

B)

Time (min)	b' (V/decade)	i_0 (mA·cm^{-2})	a
0	-0.159	1.020	-2.788
4	-0.149	1.020	-2.943
8	-0.172	1.133	-2.473
12	-0.161	1.127	-2.718
16	-0.130	1.064	-3.339
20	-0.169	1.139	-2.490

C)

Time (min)	b’ (V/decade)	i_0 (mA·cm^{-2})	A
0	-0.154	0.771	-3.510
4	-0.159	1.000	-2.993
8	-0.154	1.062	-3.030
12	-0.156	1.062	-2.976
16	-0.164	1.133	-2.724
20	-0.161	1.133	-2.795
24	-0.167	1.133	-2.670

D)

Time (min)	b' (V/decade)	i_0 (mA·cm^{-2})	a
0	-0.149	1.350	-2.986
4	-0.161	1.448	-2.582
8	-0.139	1.350	-3.150
12	-0.172	1.448	-2.325
16	-0.154	1.350	-2.764
20	-0.192	1.448	-2.070
24	-0.175	1.448	-2.334

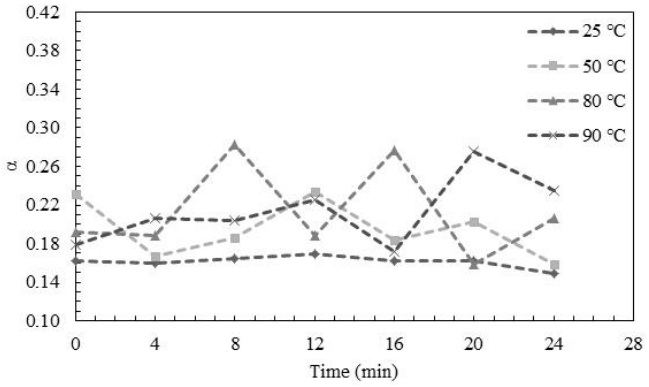

Figure 5. Comparison of charge transfer coefficient (α) at different temperatures and processing time in an aqueous 0.94 M H_3PO_4 solution.

of monoatomic hydrogen to H_2, representing the rate determining step of HER.

On other hand, the temperature promotes an increase in the HER kinetics, this result was expected from the viewpoint of the electrochemical reactions kinetics theory, however it is worth to mention that the formation of the iron phosphate coating is accelerated at higher temperatures than 25ºC, for this reason, it is probable that the iron phosphate coating can accelerate the HER kinetics, it is clearly shown at 90°C (Figure 4D). Actually it requires low energy to carry out the HER, for example the cathodic potential was -500 mV vs Ag/AgCl at 16 min and 90°C, while at 25ºC and the same processing time, the potential corresponded to -560mV vs Ag/AgCl.

When the solution temperature was controlled at 50°C, the same phenomena were observed. However, some differences in the current density were elucidated, basically it was observed that the current incremented significantly in comparison with the other tested temperatures. Moreover, the exchange current density at this temperature was the highest (1.44 mA*cm^{-2}), which means that the HER kinetics at this condition is favored (Table 3B), these results are in good agreement with the findings reported by Guiñón-Pina et.al. [10] whom found that the temperature favors the HER in the cathodic direction using different steel alloys. It was mentioned before, that iron phosphate coatings are favored when the temperature is increased, and therefore this phenomenon at 50 ºC may be related to a different coating morphology obtained under this particular condition. On the other hand, when the temperature is increased the only possible reactions that can take place during the cathodic sweep, corresponds to the hydrogen evolution and the iron electrodeposition; however, according to the Pourbaix diagram reported by Alvarado-Macías et.al. [16], the iron electrodeposition can only occur at more negative potentials than the hydrogen evolution reaction, therefore from a thermodynamic point of view, the hydrogen evolution reaction predominantly occurs.

On the other hand, when the acidity is increased to 0.94M, the charge transfer coefficient remains similar to an activationless process as can been seen in Figure 5. Furthermore the Tafel slopes b' (see Table 4) are very similar to the 0.47M condition (Table 3), therefore the electrochemical recombination of monoatomic hydrogen to H_2 is the rate determining step for the HER at 0.94M.

However, an increase in the H_3PO_4 concentration promotes a higher current density for the HER than at 0.47M. This can be clearly seen in Figure 6A at -560 mV vs Ag/AgCl. For example,

Table 4. Kinetic parameters for the electrochemical recombination rate-controlling step, employing an aqueous 0.94 M H_3PO_4 solution. A) 25°C, B) 50°C, C) 80°C, D) 90°C.

A)				**B)**			
Time (min)	b' (V/decade)	i_0 (mA·cm^{-2})	A	Time (min)	b' (V/decade)	i_0 (mA·cm^{-2})	a
0	-0.159	1.051	-3.183	0	-0.120	1.455	-3.632
4	-0.161	1.419	-2.655	4	-0.167	1.649	-2.312
8	-0.156	1.419	-2.647	8	-0.149	1.568	-2.717
12	-0.152	1.419	-2.675	12	-0.119	1.455	-3.639
16	-0.159	1.455	-2.518	16	-0.152	1.462	-2.672
20	-0.159	1.455	-2.521	20	-0.137	1.568	-2.901
24	-0.172	1.462	-2.216	24	-0.175	1.649	-2.132
C)				**D)**			
Time (min)	b' (V/decade)	i_0 (mA·cm^{-2})	A	Time (min)	b' (V/decade)	i_0 (mA·cm^{-2})	a
0	-0.159	1.455	-2.578	0	-0.175	1.455	-2.194
4	-0.161	1.350	-2.456	4	-0.152	1.455	-2.551
8	-0.108	1.221	-3.986	8	-0.154	1.492	-2.385
12	-0.161	1.455	-2.337	12	-0.139	1.455	-2.688
16	-0.110	1.221	-3.850	16	-0.182	1.649	-1.878
20	-0.192	1.492	-1.840	20	-0.114	1.284	-3.480
24	-0.147	1.350	-2.685	24	-0.133	1.350	-2.877

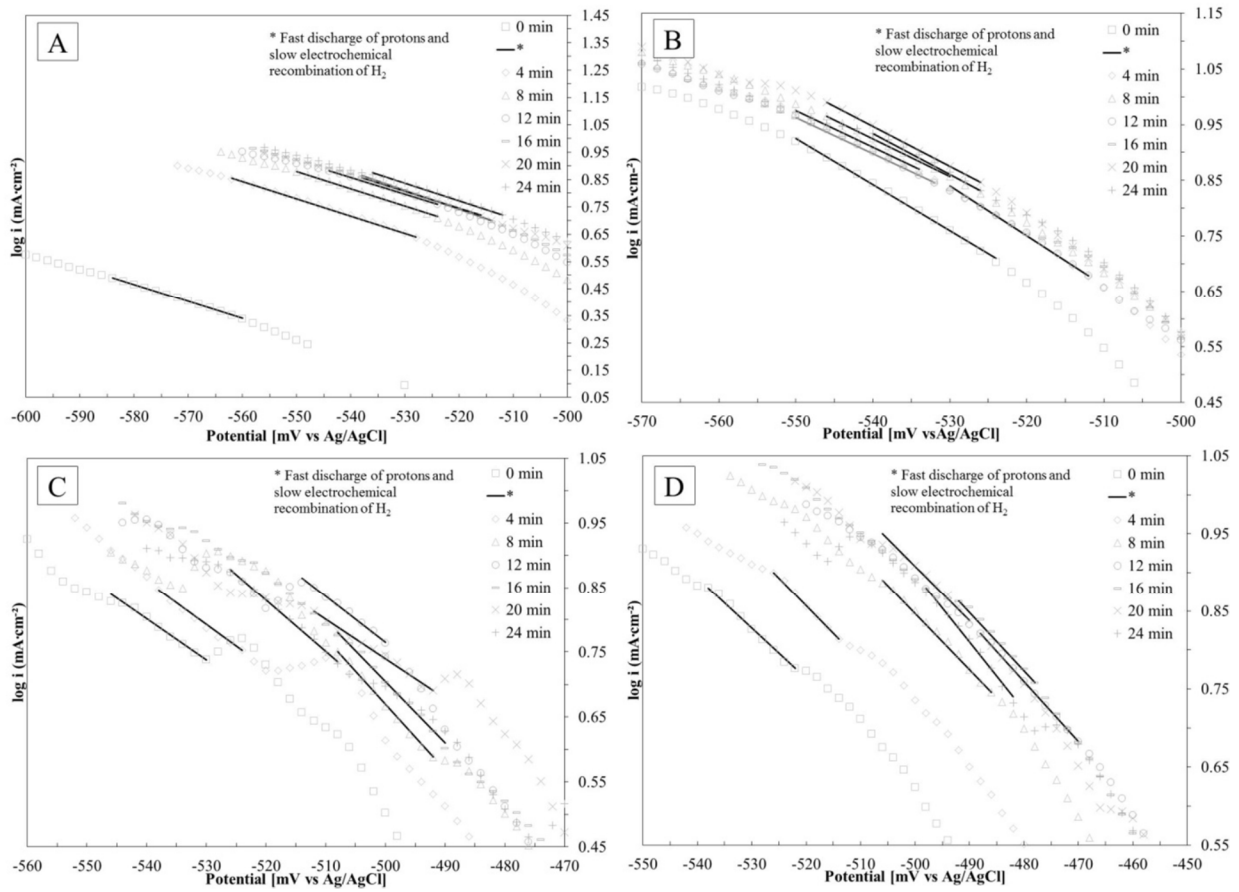

Figure 6. Comparison of the cathodic polarization curves for immersion of steel in an aqueous H_3PO_4 solution at A)25°C, B)50°C, C)80°C, D)90°C. All experiments employed 0.94 M H_3PO_4. The polarization curves were recorded every 4 minutes during the immersion process.

the current density increased around 0.35mA·cm^{-2} at the beginning of the phosphatizing process, in comparison with the Figure 4A at -560 mV, where the current density was around 0.10mA·cm^{-2}. Furthermore the exchange current densities for this acid concentration at different temperatures were higher (see Table 4) than the 0.47M concentration (see Table 3). It was also observed that the current density was favored when the temperature was raised up to 90ºC.

Figure 6 shows the cathodic polarization curves for the four tested temperatures, it is possible to see in all immersion times at 50°C and -570 mV vs Ag/AgCl, the highest current density recorded was around 1.00mA·cm^{-2}, for that reason this temperature could be a good condition for improving the HER kinetics. However, when the temperature was increased to 90ºC, the potential or energy required to carry out the H_2 production is lowered (Fig 6D).

Until this moment, it has been showed the effect of employing different phosphatizing solutions on the HER, and it was proposed the iron phosphate coatings as a detrimental factor to increase the hydrogen evolution reaction kinetics. Furthermore in the last Figures it was mentioned that the coating morphology plays an important role in the HER kinetics. Actually, Alvarado-Macías et al (2013) revealed a continuous change of the coating morphology during the immersion time, i.e. the layer nature can be porous or even uniform [16].

As can be seen in Figure 7, the morphology of the coating on the steel presents craters in the entire surface, which can be associated to the continuous evolution of hydrogen bubbles. The chemical composition also shows this coating is predominantly formed by iron phosphate with a small part of manganese and chrome. It is relevant to mention manganese and chrome are contained in the steel and not in the solutions of Figures 4 and 6; therefore, the EDXS analysis registered these chemical elements. Therefore, this micrograph can show that hydrogen can be produced on iron phosphate surfaces. Actually these results are in good agreement with the findings reported by Alvarado-Macías et.al. [16].

3.2.Effect of the temperature and Mn ions in solution on the H_2 evolution kinetics

On the other hand, the effect of Mn ions in solution was tested on the HER kinetics, using the same acidity 0.94 M H_3PO_4 at pH 1 and 25 or 90ºC. Figure 8, revealed similar charge transfer coefficients behaving as an activationaless process, which suggests low activation energy for the HER. The Tafel plots presented in Table 5 are characteristic for the same mechanism: the fast discharge of monoatomic hydrogen and a slow electrochemical recombination of H_2.

Figure 9, shows the polarization curves for this manganese solution, the results revealed that Mn in solution had a catalytic effect

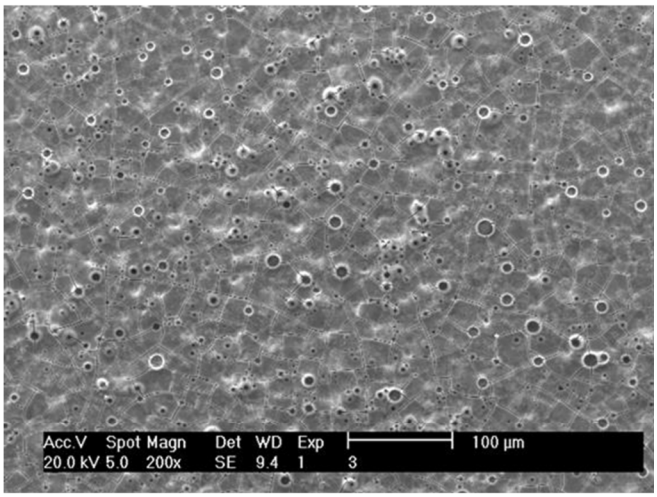

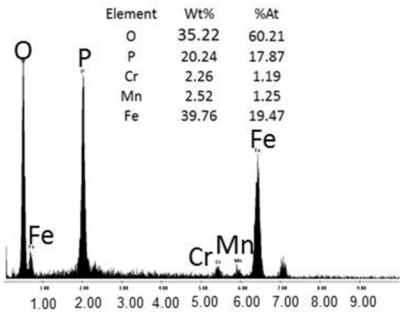

Figure 7. Microstructural characterization and chemical composition of the iron phosphate coating employing a phosphatizing solution with 0.94 M H_3PO_4 at 90°C

on the hydrogen generation rate at room temperature and the coating formed on the steel was iron phosphate, actually when the temperature was increased up to 90°C the generation rate was favored. Furthermore the exchange current densities for these experiments (Table 5) were the highest when they are compared with that of Table 4, i.e. without the presence of Mn in solution.

For that reason, a possible mechanism proposed is the next: the manganese ions acts as a catalyst for the HER production due to the Tafel slopes obtained in each experiment (at room temperature and

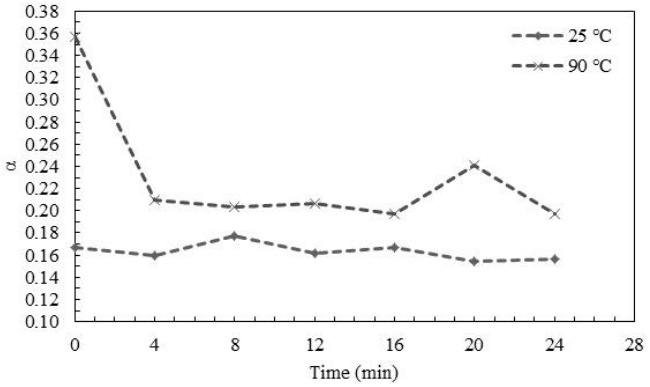

Figure 8. Comparison of charge transfer coefficient (α) at different temperatures and processing time in an aqueous H_3PO_4-Mn solution; 0.94M H_3PO_4, pH=1.

90°C) are similar to that obtained by Fuentes-Aceituno and Lapidus (2012) [5], in this work the authors found a catalytic effect of the ferrous ions contained in acid solutions for the HER generation; it is important to remember that the chemical elements such as the Fe and Mn are transition metals and have similar chemical properties. Therefore, it is possible that Mn ions has the similar catalytic effect found with ferrous ions on the HER.

This catalytic effect can be clearly observed by comparing the cathodic polarization curves of the solution C at 25°C (Figure 9A) with the curves of the solution B at the same temperature (Figure 6A). For example, if the cathode potential is held at -520 mV vs Ag/AgCl, it can be observed an increment in the current density at 24 min, i.e. the Figure 6A has 0.75mA·cm^{-2} approximately; however in the presence of Mn in solution the current density was increased to 0.90mA·cm^{-2} (Figure 9A). It can be also observed at the end of the immersion time (Figure 6A), that the potential became more negative in comparison with that of Figure 9A and this represents a higher energy consumption to produce H_2 without manganese than with the presence of manganese ions. On the other hand, the catalytic effect of manganese ions on the HER kinetics can be also observed at 90ºC (Figure 9B). Actually, the current density recorded for a solution with manganese was higher than that for a solution without manganese, for example with a fixed potential of -520 mV vs Ag/AgCl and 12 min of immersion time, the current

Table 5. Kinetic parameters for the electrochemical recombination rate-controlling step, employing an aqueous H_3PO_4-Mn solution; 0.94M H_3PO_4. A) 25°C, B) 90°C.

A)				**B)**			
Time (min)	b' (V/decade)	i_0 (mA·cm^{-2})	A	Time (min)	b' (V/decade)	i_0 (mA·cm^{-2})	a
0	-0.154	1.127	-3.048	0	-0.088	1.284	-4.852
4	-0.161	1.455	-2.460	4	-0.149	1.649	-2.403
8	-0.145	1.455	-2.764	8	-0.154	1.649	-2.302
12	-0.159	1.462	-2.394	12	-0.152	1.649	-2.332
16	-0.154	1.455	-2.474	16	-0.159	1.665	-2.207
20	-0.167	1.568	-2.208	20	-0.130	1.284	-2.982
24	-0.164	1.568	-2.249	24	-0.159	1.492	-2.304

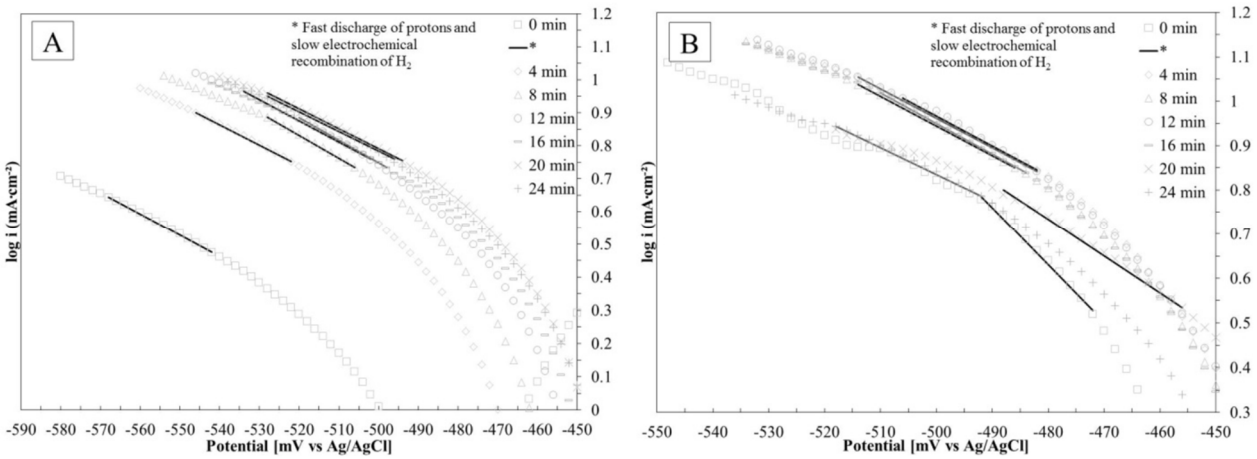

Figure 9. Comparison of the cathodic polarization curves for immersion of steel in an aqueous H_3PO_4-Mn solution at A) 25°C, B) 90°C. All experiments employed 0.94 M H_3PO_4 and Mn. The polarization curves were recorded every 4 minutes during the immersion process.

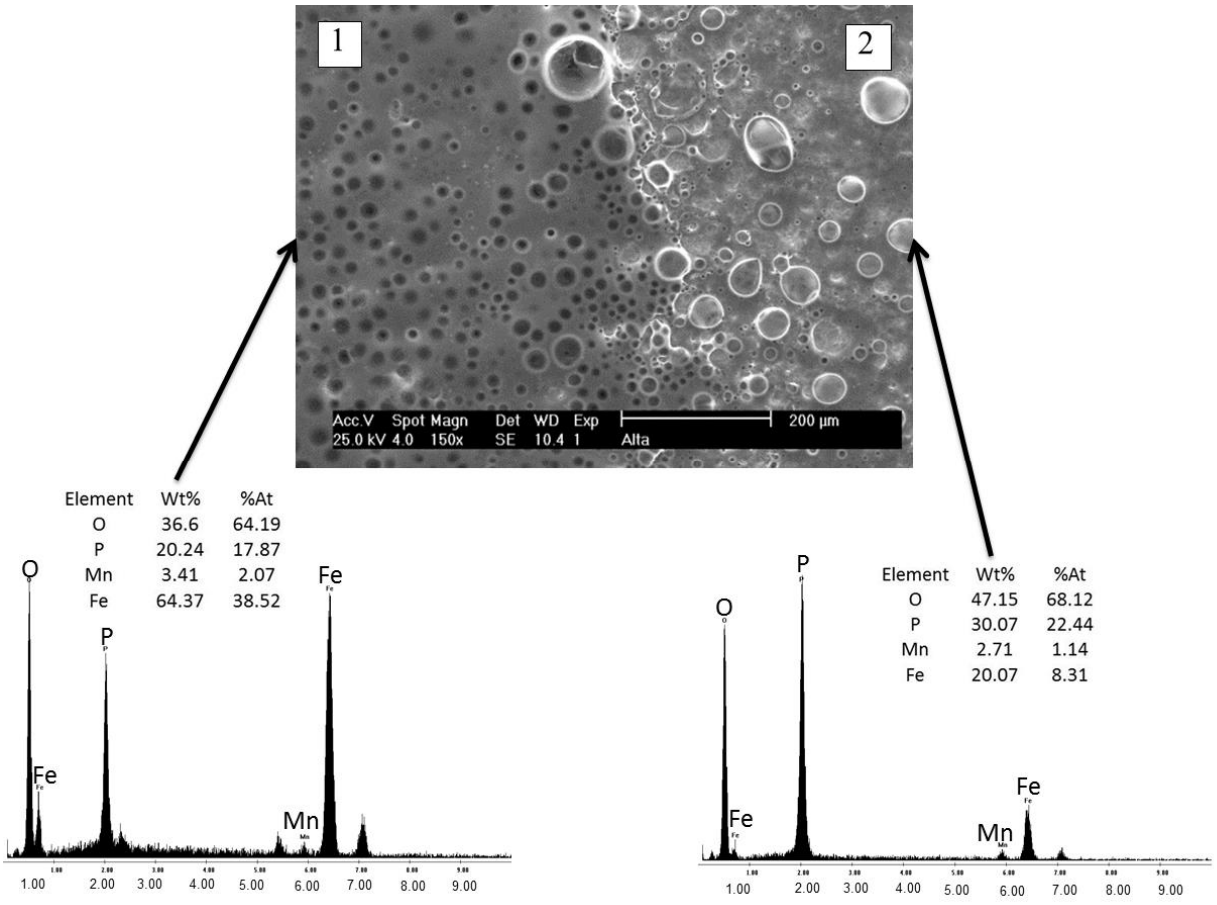

Figure 10. Microstructural characterization and chemical composition of the iron phosphate coating employing a phosphatizing solution with 0.94M H_3PO_4 and Mn in solution at 90°C. 1) Porous Layer, 2) Less Porous Uniform Layer.

density was around 0.95mA·cm^{-2} (see Figure 6D), on the other hand, the presence of manganese promotes an increase in the current value around 1.05mA·cm^{-2} (see Figure 9B).

Figure 10 displays the microstructural characterization and the chemical composition of the iron phosphate coating during the hydrogen evolution experiments. The iron phosphate coating pre-

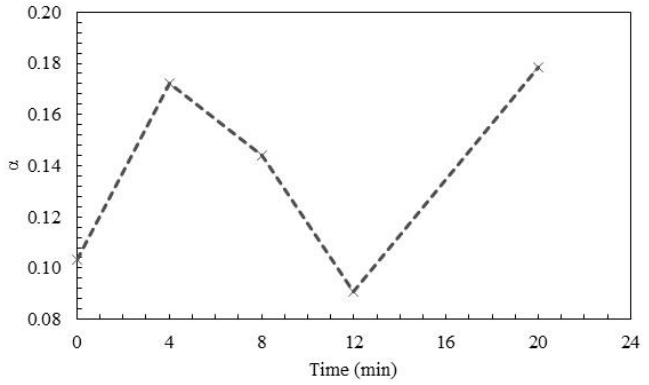

Figure 11. Comparison of the charge transfer coefficient (α) at different processing time on a manganese phosphate coating at 90°C.

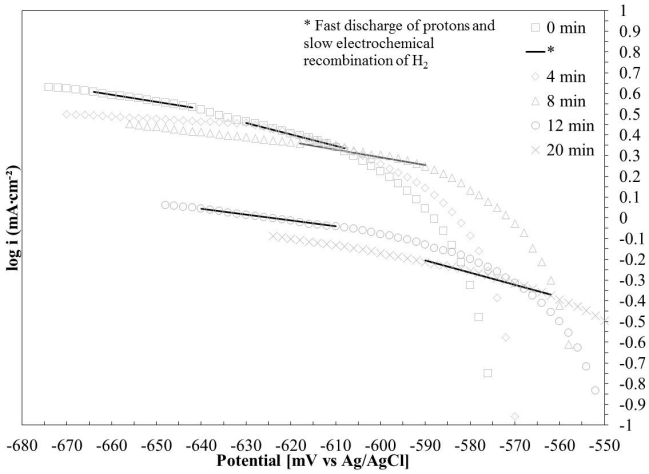

Figure 12. Comparison of the cathodic polarization curves for immersion of steel with a manganese phosphate coating at 90°C. The experiment employed 0.94 M H_3PO_4. The polarization curves were recorded every 4 minutes during the immersion process.

sented more craters than that of Figure 7, it is important to remember that the craters were related to the generation of hydrogen bubbles on the coating surface. Therefore, this Figure 10, shows an increase in the number of craters or holes, so it is indicative the HER is promoted under this condition. In addition to the last, two different types of morphology are shown; 1) a porous layer and 2) a less porous uniform layer, probably these differences can be associated to the different composition of the iron phosphate layers. It is worth to mention that Mn was found in both EDXS analysis shown in Figure 10; this Mn as was mentioned before in Figure 7 can be related to the Mn contained in the steel sample.

3.3. Effect of the manganese phosphate coating on the H_2 evolution kinetics

Finally when the manganese phosphate coating was tested on steel, the results showed that the hydrogen generation was decreased considerably in comparison with the iron phosphate coatings. Figure 11, displays the charge transfer coefficients for a phosphatizing solution containing 0.94M H_3PO_4, 0.6M Mn and 0.2M HNO_3 (as a catalyst for the manganese phosphate generation), it is interesting to note that the charge transfer coefficients were very similar to that of Figure 3, 5 and 8, which are related to an activationless process. Actually the Tafel slopes recorded at different immersion times (Table 6) showed that a different HER mechanism is occurring at lower generation rates than with the iron phosphate coatings. Furthermore, it is possible to observe the current density decreased drastically during the immersion time (see Figure 12), i.e. the current density was 0.6mA·cm^{-2} at -670 mV vs Ag/AgCl and 0 min, while at the end (20 min) the current reached a value of -0.1mA·cm^{-2} at -620 mV vs Ag/AgCl, this suggests that HER was inhibited. Actually the exchange current density at 12 and 20 minutes decreased greatly (Table 6) in comparison with any condition tested in this research. On the other hand, Figure 12 shows the necessity to apply a more negative potential to activate the HER than the other conditions showed in Figure 9B, indicating an increase in the energy consumption.

Table 6. Kinetic parameters for the electrochemical recombination rate-controlling step, employing a manganese phosphate coating at 90°C.

Time (min)	b' (V/decade)	i_0 (mA·cm^{-2})	a
0	-0.303	1.363	-1.607
4	-0.182	1.116	-2.980
8	-0.217	1.116	-2.488
12	-0.345	0.795	-1.820
20	-0.175	0.560	-3.593

4. CONCLUSIONS

In this research, cathodic polarization experiments were performed in order to study the nature of the hydrogen evolution reaction mechanism on steel with different types of phosphatizing solutions by varying the acidity, temperature, immersion time, coating (iron or manganese phosphate) with or without Mn ions in solution.

The Tafel plots of the phosphatizing process revealed one electrical potential zone where the monoatomic hydrogen is recombined electrochemically to H_2 as the rate determining step, with charge transfer coefficients similar to an activationless process.

Another important factor in the HER kinetics is the temperature; it was found that an increase in temperature up to 90ºC helps to produce more hydrogen than at 25ºC. On the other hand, a temperature of 50°C employing either 0.47 or 0.94M H_3PO_4 at pH 1 promotes an increase in the current density due to the formation of an iron phosphate coating on the steel cathode. The formation of $FePO_4$ on steel promotes the highest rate for the electrochemical recombination of monoatomic hydrogen to H_2.

Furthermore an increase in the acidity causes a higher exchange current density that benefits the hydrogen generation rate. The microstructural characterizations revealed that the coating morphology is an important factor in the hydrogen generation, i.e. the HER is favored on the porous iron phosphate coatings.

On the other hand, it was found a catalytic effect on the hydro-

gen generation rate at room temperature, when Mn ions were incorporated to the solution at pH 1. This catalytic effect is more efficient when the temperature was increased up to 90°C. Finally it was also observed that the manganese phosphate coating decreases the HER kinetics at pH 2.57 and 90ºC.

5. ACKNOWLEDGEMENTS

Gabriela Alvarado Macías is grateful to CONACyT (México) for the postgraduate scholarship received. Also, the collaboration of Felipe Márquez, Socorro García and Teodoro Caballero in this investigation is duly recognized.

REFERENCES

[1] A. Abbaspour, E. Mirahmadi, Fuel, 104, 575 (2013).
[2] A. Phuruangrat, D. Ham, S. Thongtem, Electrochemistry Communications, 11, 1740 (2009).
[3] R.K. Shervedani, A.R. Madram, Electrochim. Acta, 53, 426 (2007).
[4] W. Xu, C. Liu, W. Xing, T. Lu, Electrochem. Commun., 9, 180 (2007).
[5] J.C. Fuentes-Aceituno and G.T. Lapidus, J. New Mat. Electrochem. Systems, 15, 225 (2012).
[6] A. Abbaspour, F. Norouz-sarvestani and E. Mirahmadi, Electrochimica Acta, 76, 404 (2012).
[7] M.S. El-Deab, Mahmoud M. Saleh, Int. J. Hydrogen Energy, 28, 1199 (2003).
[8] S. Sharifi-Asla, and D.D. Macdonaldb, Journal of the Electrochemical Society, H382 (2013).
[9] J. Liu, H. Watanabe, M. Fuji, M. Takahashi, Electrochemistry Communications, 11, 107 (2009).
[10] V. Guiñón-Piña, A. Igual-Muñoz, and J. García-Antón, International Journal of Electrochemical Science, 6123 (2011).
[11] M.H. Moayed, N.J. Laycock, and R.C. Newman, Corrosion Science, 45, 1203 (2003).
[12] P.T. Jakobsen and E. Maahn, Corrosion Science, 43, 1693 (2001).
[13] A. Igual Muñoz, J. García Antón, J.L. Guiñón, V. Pérez Herranz, Corrosion Science,. 48, 4127 (2006).
[14] L.F. Garfias-Mesias, J.M. Sykes, and C.D.S. Tuck, Corrosion Science, 38, 1319 (1996).
[15] N.J. Laycock, M.H. Moayed, and R.C. Newman, Journal of the Electrochemistry Society, (1998).
[16] G. Alvarado-Macías, J.C. Fuentes-Aceituno, A. Salinas-Rodríguez, F.J. Rodríguez-Varela, J. Mex. Chem. Soc., 57, 328 (2013).
[17] L.I. Krishtalik, in "Charge Transfer Reactions in Electrochemical and Chemical Processes", 1st Edition, Consultants Bureau New York, Ed., U.S.A., 1986, pp. 26-67.